Available online at www.sciencedirect.com
SCIENCE DIRECT®
Physica B 371 (2006) 245–248
PHYSICA B
www.elsevier.com/locate/physb

The behavior of photoinduced charge delocalization in bilayer manganite $LaCa_2Mn_2O_7$

J.M. Dai[a,b,*], G.Y. Yuan[a], W.H. Song[b], Y.P. Sun[b]

[a]*Department of Physics, Huaibei Coal Teachers' College, Huaibei 235000, PR China*
[b]*Key Laboratory of Materials Physics, Institute of Solid State Physics, Academia Sinica, Hefei 230031, PR China*

Received 21 August 2005; received in revised form 7 October 2005; accepted 7 October 2005

Abstract

The properties of electrical and magnetic transport in bilayer perovskite manganite $LaCa_2Mn_2O_7$, were investigated by the measurements of resistivity and magnetization. A distinct increasing in resistivity at low temperatures, which is in good agreement with an obvious decreasing in magnetization at the corresponding temperature region was observed. It was suggested that the sample undergoes a transition from ferromagnetic metallic to charge localization state caused by the antiferromagnetic charge ordering (CO). The behavior of photoinduced charge delocalization was observed under irradiation of He–Ne laser (632.8 nm) at the low temperatures. It can be explained in terms of the effect of photoinduced charge transfer from O-2p to Mn^{4+}-3d e_g orbital state resulting in the partial melting of CO state.

PACS: 75.30.kz; 71.30.+h; 75.30.−m

Keywords: Delocalization; $LaCa_2Mn_2O_7$; Photoinduced

1. Introduction

Recently, the photoinducing (also called photodoping) methods are widely used to investigate in perovskite manganites $R_{1-x}A_xMnO_3$ (where R and A are trivalent and divalent ions, respectively). Many interesting phenomena [1–7], such as photoinduced persistent photoconductivity (PPC) and photoinduced metal-insulator transition in Pr-based manganites [1,2], have been found. In our previous works, we have found the behavior of coexistence of PPC effect and ordinary photoconductivity in the films of $(La_{0.3}Nd_{0.7})_{2/3}Ca_{1/3}MnO_3$ induced by visible-light with different wavelengths [8], and the temperature of appearance of PPC can be elevated through the magnetic coupling in multilayer films [9]. The investigations of photoinduced effects are very beneficial to understand the physical mechanism of colossal magnetoresistance (CMR) effect and related properties existing in the perovskite manganites. However, so far, the large number of photoinducing studies are performed on manganites with the structure of ABO_3 and little attention is paid to the layered perovskite manganites $R_{n-nx}A_{1+nx}Mn_nO_{3n+1}$ ($n = 1$, 2, etc).

Compared with the ABO_3-type manganites, the layered manganites also exhibit CMR effect, which are widely studied for structural, magnetic, transport properties [10–20]. However, the layered manganites reveal a more delicate balance between ferromagnetic (FM) double exchange and antiferromagnetic (AF) superexchange interaction because of their reduced dimensionality. Therefore, the ground state behavior of the layered manganites may display sensitive properties to external stimulation, which should be studied by photoinducing experiments.

In this work, we present the studies on electrical and magnetic transport properties, as well as the photoinduced effect in the bilayer ($n = 2$) manganite $LaCa_2Mn_2O_7$. For the doped manganites with $x = 0.5$, because of its equal amounts of Mn^{3+} and Mn^{4+} ions, it should be more sensitive in transport properties to external stimulation [13,14,20].

*Corresponding author. Key Laboratory of Materials Physics, Institute of Solid State Physics, Academia Sinica, Hefei 230031, PR China.
E-mail address: jmdai@issp.ac.cn (J.M. Dai).

0921-4526/$ - see front matter © 2005 Elsevier B.V. All rights reserved.
doi:10.1016/j.physb.2005.10.114

2. Experiment

The polycrystalline sample of $LaCa_2Mn_2O_7$ was prepared by means of a sol–gel method as reported previously [21]. The phase purity of the sample was examined by powder X-ray diffraction. The magnetization as a function of temperature was measured by using a commercial superconducting quantum interference device magnetometer (SQUID). The resistivity was measured by a standard four-probe method in the temperature range from 15 to 300 K obtained by means of a Cryogenic Refrigeration equipment. An iron-doped gold vs. chrome thermocouple with an accuracy of 0.1 K was used to measure the temperature of the sample. To avoid the influence of bolometric effect, the rate of cooling and warming was strictly controlled by a digital temperature controller device. A He–Ne laser (632.8 nm) with 28 mW output power, whose power fluctuation was no more than 5%, was used to irradiate the sample. The laser beam was coupled to the sample-room by a beam splitter and a quartz glass window, and the diameter of laser spot illuminated on the sample surface was about 8 mm with the power of 22 mW. The beam splitter together with a photodetector was used to monitor and adjust the laser power. The dimension of the sample is about $4 \times 3 \times 0.4\,mm^3$ with polished surface.

3. Results and discussion

X-ray diffraction pattern indicates that the sample of $LaCa_2Mn_2O_7$ is single phase with the $Sr_3Ti_2O_7$-type tetragonal perovskite structure (I4/mmm). The temperature dependence of magnetization (M–T) measured in field cooled (fc) state at $H = 100$ G is shown in Fig. 1. The magnetic transition temperature T_C determined by the maximum slope criterion of the M–T curve is 231 K. The sample is paramagnetic (PM) above the T_C, while it is FM below T_C. The magnetization exhibits a gradual increase with the decreasing of temperature in FM region. However the magnetization has a distinct drop at temperature below ~30 K, which is in good agreement with an obvious increasing in resistivity shown in Fig. 2 (the curve 1). The inset in Fig. 1 shows the temperature dependence of magnetoresistance ($MR = ((\rho_0 - \rho_H)/\rho_0) \times 100\%$) with an applied magnetic field of 5000 G. The sample exhibits a behavior of large MR, which is similar to the previous reports [11]. Fig. 2 shows the temperature dependence of the resistivity ($\rho - T$) under the conditions of no-laser (the curve 1) and laser (the curve 2) irradiation. It indicates that the sample exhibits a semiconductive behavior at high temperature region over the peak temperature of the resistivity of T_P~93 K and a metallic behavior in the temperature range from 93 to 35 K. The resistivity reaches a valley point at T_V~35 K and there appears a rapid increase at temperature below ~30 K. The behaviors of magnetic and electrical transport at low temperature suggest that the sample undergoes a transition from FM metallic to AF charge ordering (CO) state at the temperature about T_{CO}~30 K. A large amount of studies indicate that the perovskite manganites, both of ABO_3-type [22] and layered structure [13,14], often display the coexistence of FM conducting and CO insulating states in the intermediate doped region (with equal amounts of Mn^{3+} and Mn^{4+} ions). Because of the existence of two types of magnetic ordering interaction in layered manganites caused by the anisotropic carrier transport and exchange interaction [11], and long-range electron Coulomb interaction, the competition between them at low temperatures can give rise to the ordering arrangement of Mn^{3+} and Mn^{4+} ions in real space [13,14], resulting in the emergence of charge localization.

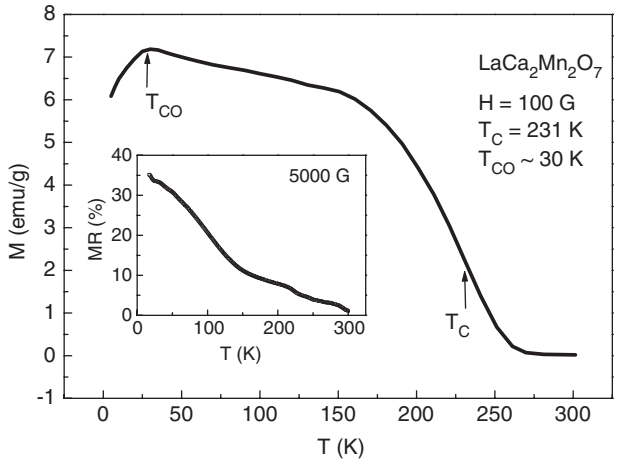

Fig. 1. The field-cooled magnetization as function of temperature. The inset shows the temperature dependence of magnetoresistance ($MR = ((\rho_0 - \rho_H)/\rho_0) \times 100\%$) with a magnetic field of 5000 G.

The phenomenon that T_P~93 K is far from the magnetic transition temperature T_C~231 K is considered a common feature existing in polycrystalline samples of layered manganites, which is attributed to the anisotropic carrier transport mentioned above. It is noted that some properties measured in our samples, such as the value of T_C and the electrical transport at low temperatures, are slightly different from those of the samples reported in Ref. [11], which may originate from the different process of the sample preparation between the solid state reaction and the sol–gel method.

To clarify the conduction mechanism exhibited in this material, three different models which are variable-range hopping [23], semiconductor transport [24] and the small-polaron hopping [25], are used to fit the curve of ρ–T obtained in this experiment. The results indicate that the small-polaron hopping with the formula $\rho = \rho_0 T \exp(E_a/k_B T)$ gives a better fitting at high temperature PM region, where the E_a is the activation energy of small-polaron hopping, the k_B is the Boltzmann constant. However, in the low temperature range below T_{CO}~30 K, the conduction mechanism can be described according to the variable-range-hopping model with the formula $\rho = \rho_0 \exp(T_0/T)^{1/4}$ as shown in the inset (a) in Fig. 2, in which

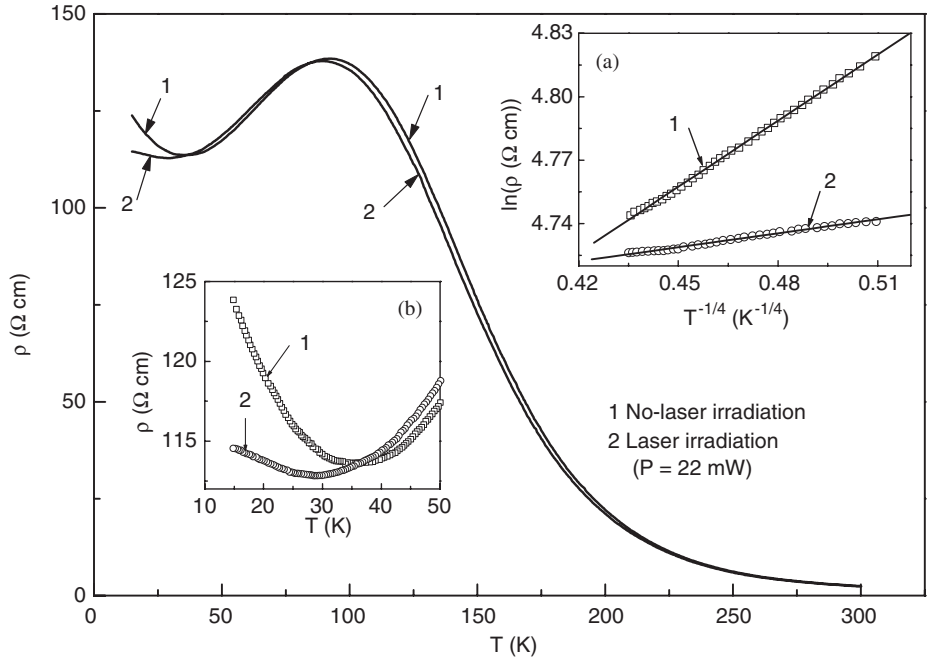

Fig. 2. Temperature dependence of resistivity (ρ–T) under the conditions of no-laser irradiation (curve 1) and laser irradiation (curve 2). The inset (a) shows the ρ–T curve replotted in the form $\ln \rho - T^{-1/4}$ at temperatures below 28 K (the solid lines are fitting results.). The inset (b) shows magnification of ρ–T at the low temperatures near T_V.

is observed the transport behavior of charge localization corresponding to the AF–CO state. In the inset (a), the open symbols show the ρ–T curve replotted in the form $\ln \rho - T^{-1/4}$ at the temperatures below ~30 K, and the solid lines are the results of linear fitting.

Under the laser irradiation, the property of electrical transport shown in Fig. 2 (the curve 2) reveals some dramatic changes. First, the T_P shifts slightly to lower temperature from 93 to 90.5 K, and the T_V shifts from 35 to 28 K. Secondly, the resistivity decreases in the semiconducting region and increases slightly in the metallic region. Thirdly, the resistivity has a distinct decreasing in the AF–CO region. The fitting results of $\ln \rho - T^{-1/4}$ shown in the inset (a), can be expressed as $\ln \rho = 4.2884 + 1.0423T^{-1/4}$ with correlation coefficient $R = 0.9996$ for curve 1, and $\ln \rho = 4.6298 + 0.2201T^{-1/4}$ with the $R = 0.9963$ for curve 2, respectively. The changes in the slope values and the correlation coefficients (R) of the fitting lines under no-laser irradiation and laser irradiation just imply the different transports in the CO state and the behavior of charge delocalization under laser irradiation. In our previous works [9], the heating effect can cause the temperature rise with about 2 K on the surface of sample under the continuous laser illumination of ~26 mW. However, the distinct difference in the shifts of T_P and T_V under laser illumination mentioned above cannot be completely explained as heating effect.

The inset (b) in Fig. 2 shows the magnification of ρ–T curve at low temperature region near the T_V, in which the photoinduced resistivity change can be observed more clearly. Here, we define the photoinduced resistivity $\Delta\rho_L$ as $\rho_L - \rho$, where ρ_L and ρ are the resistivity under laser irradiation and no-laser irradiation, respectively. The $\Delta\rho_L$ as a function of temperature is shown in Fig. 3. It can be observed that the $\Delta\rho_L$ is negative and positive in the semiconducting and metallic region, respectively, and the negative $\Delta\rho_L$ is much larger in AF–CO region. The inset in Fig. 3 shows the variation of $\Delta\rho_L$ under different laser power (P) at the temperature of 15 K. It indicates that the curve of the $\Delta\rho_L - P$ is nonlinear, and the $\Delta\rho_L$ does not reach saturation even if the laser power illuminated on the sample is more than 26 mW.

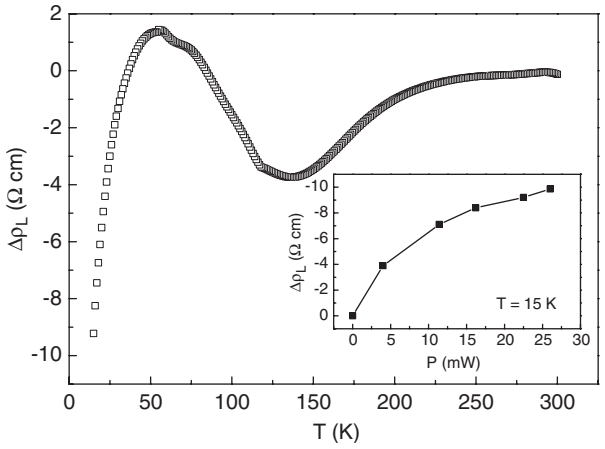

Fig. 3. Temperature dependence of photoinduced resistivity $\Delta\rho_L = \rho_L - \rho$. The inset shows the variation of $\Delta\rho_L$ under different laser power (P) at the temperature 15 K.

As to the slight shift of T_P, and the resistivity change at temperatures above ~30 K under the laser irradiation, it can mainly be ascribed to heating effect due to the

continuous laser illumination mentioned above. However, the intriguing phenomenon is that the resistivity decreases distinctly in the AF–CO region under the laser irradiation as shown in Figs. 2 and 3, which can be explained briefly according to the photoinduced charge transfer from O-2p to Mn^{4+}-3d e_g orbital state resulting in the partial melting of CO state.

From the investigation of optical conductivity spectra $\sigma(\omega)$ in the analogous manganites ($La_{2-2x}Sr_{1+2x}Mn_2O_7$, $x = 0.4$) [26], the spectra show an onset around 3 eV and peaking at 4 eV. This peak can be assigned to a charge-transfer-type transition from O-2p to Mn-t_{2g}-like states. The spectra with a broad peak below 3 eV are dominated by intraband and interband transitions relevant to O-2p to Mn-e_g-like states, which can disturb the regular ordering of Mn^{3+} and Mn^{4+} in real space. So the strong charge localization caused by the CO interaction can be "melted" by the photon irradiation, resulting in the decrease of resistivity. However, comparing with our previous studies in ABO_3-type manganites with cluster-glass state [8], the photon energy of 1.9 eV used in this experiment resulting in the melting of CO state is far lower than ~3 eV, which just indicates the variation of electronic structures and the anisotropic interaction due to the reduced dimensionality in layered manganites. Furthermore, because of the limit of penetration depth of the photon irradiation, the photo-induced effect is surface effect for the sample studied in this work. The photoinduced charge delocalization can be understood as a partial or local "melting" of CO phase just on the surface not in the whole of the sample. It should be more interesting and important in potential application such as optical switch to study in single crystal and epitaxial film samples, which may obtain more obvious photoindued effects with anisotropic properties. This work is in progress.

4. Conclusion

The complex behaviors of electrical and magnetic transport have been observed in the bilayer manganite $LaCa_2Mn_2O_7$. The sample undergoes a transition from FM metallic to AF–CO state at low temperatures, which can be understood as the result of the competition between the anisotropic magnetic ordering interaction accompanying long-range electron Coulomb interaction. The behavior of photoinduced charge delocalization is observed under irradiation of He–Ne laser in the AF–CO state region. It can be explained in terms of the effect of photoinduced charge-transfer from O-2p to Mn^{4+}-3d e_g orbital state resulting in the partial melting of CO state.

Acknowledgement

This work was supported by National Key Research under Contact no. 001CB610604, and the National Nature Foundation of China under Contract no. 10374033, Ministry of Education, Anhui Province Grant no. 2002kj253ZD.

References

[1] V. Kiryukhin, D. Casa, J.P. Hill, B. Keimer, A. Vigliante, Y. Tomioka, Y. Tokura, Nature (London) 386 (1997) 813.
[2] K. Miyano, T. Tanaka, Y. Tomioka, Y. Tokura, Phys. Rev. Lett. 78 (1997) 4257.
[3] M. Fiebig, K. Miyano, Y. Tomioka, Y. Tokura, Science 280 (1998) 1925.
[4] Y. Okimoto, Y. Tomioka, Y. Onose, Y. Otsuka, Y. Tokura, Phys. Rev. B 59 (1999) 7401.
[5] M. Sasaki, G.R. Wu, W.X. Gao, H. Negishi, M. Inoue, G.C. Xiong, Phys. Rev. B 59 (1999) 12425.
[6] H. Oshima, M. Nakamura, K. Miyano, Phys. Rev. B 63 (2001) 075111.
[7] Y. Okimoto, Y. Ogimoto, M. Matsubara, Y. Tomioka, T. Kageyama, T. Hasegawa, H. Koinuma, M. Kawasaki, Y. Tokura, Appl. Phys. Lett. 80 (2002) 1031.
[8] J.M. Dai, W.H. Song, J.J. Du, J.N. Wang, Y.P. Sun, Phys. Rev. B 67 (2003) 144405.
[9] J.M. Dai, W.H. Song, S.G. Wang, K.Y. Wang, S.L. Ye, J.J. Du, Y.P. Sun, J. Appl. Phys. 89 (2001) 6967;
J.M. Dai, W.H. Song, S.G. Wang, K.Y. Wang, S.L. Ye, J.J. Du, Y.P. Sun, J. Appl. Phys. 90 (2001) 3118.
[10] Y. Moritomo, A. Asamitsu, H. Kuwahara, Y. Tokura, Nature 380 (1996) 141.
[11] H. Asano, J. Hayakawa, M. Matsui, Phys. Rev. B 56 (1997) 5395;
H. Asano, J. Hayakawa, M. Matsui, Phys. Rev. B 57 (1998) 1052.
[12] T. Kimura, R. Kumai, Y. Tokura, J.Q. Li, Y. Matsui, Phys. Rev. B 58 (1998) 11081.
[13] Y. Murakami, H. Kawada, H. Kawata, M. Tanaka, T. Arima, Y. Moritomo, Y. Tokura, Phys. Rev. Lett. 80 (1998) 1932.
[14] J.Q. Li, Y. Matsui, T. Kimura, Y. Tokura, Phys. Rev. B 57 (1998) R3205.
[15] T. Nachtrab, S. Heim, M. Mößle, R. Kleiner, O. Waldmann, R. Koch, P. Müller, T. Kimura, Y. Tokura, Phys. Rev. B 65 (2001) 012410.
[16] K.V. Kamenev, M.R. Lees, G. Balakrishnan, D. McK. Paul, W.G. Marshall, V.G. Tissen, M.V. Nefedova, Phys. Rev. Lett. 84 (2000) 2710.
[17] J.Q. Li, C. Dong, L.H. Liu, Y.M. Ni, Phys. Rev. B 64 (2001) 174413.
[18] H. Zhu, X.M. Liu, K.Q. Ruan, Y.H. Zhang, Phys. Rev. B 65 (2002) 104424.
[19] R.L. Zhang, W.H. Song, Y.Q. Ma, J. Yang, B.C. Zhao, Z.G. Sheng, J.M. Dai, Y.P. Sun, Phys. Rev. B 70 (2004) 224418;
R.L. Zhang, W.H. Song, Y.Q. Ma, J. Yang, B.C. Zhao, Z.G. Sheng, J.M. Dai, Y.P. Sun, J. Appl. Phys. 96 (2004) 4965.
[20] R. Seshadri, A. Maignan, M. Hervieu, N. Nguyen, B. Raveau, Solid State Commun. 101 (1997) 453.
[21] T. Yu, W. Song, K. Wang, S. Wang, Y. Sun, Phys. Stat. Sol. (a) 172 (1999) 451.
[22] M. Roy, J.F. Mitchell, A.P. Ramirez, P. Schiffer, Phys. Rev. B 58 (1998) 5185.
[23] N.F. Mott, Adv. Phys. 21 (1972) 785.
[24] M. Jaime, M.B. Salamon, K. Pettit, M. Rubinstein, R.E. Treece, J.S. Horwitz, D.B. Chrisey, Appl. Phys. Lett. 68 (1996) 1576.
[25] D.C. Worledge, G.J. Snyder, M.R. Beasley, T.H. Geballe, J. Appl. Phys. 80 (1996) 5158;
D.C. Worledge, L. Miéville, T.H. Geballe, Phys. Rev. B 57 (1998) 15267.
[26] Y. Okimoto, Y. Tokura, J. Supercon. 13 (2000) 271.